CGU HS Committee on River Ice Processes and the Environment
13th Workshop on the Hydraulics of Ice Covered Rivers
Hanover, NH, September15-16, 2005

The Effects of River Ice on Scour and Sediment Transport

MAJ Decker B. Hains[1], Ph.D., P.E. and Leonard J. Zabilansky[2], P.E.

[1] *Assistant Professor, Department of Civil and Mechanical Engineering, United States Military Academy, West Point, NY 10996, decker.hains@usma.edu*

[2] *Civil Engineer, U.S. Army Cold Regions Research and Engineering Laboratory (CRREL), Engineer Research and Development Center (ERDC), Hanover, New Hampshire 03775-1290, Leonard.J.Zabilansky@erdc.usace.army.mil*

ABSTRACT

Field observations indicate ice covers significantly affect sediment transport processes in rivers, especially scour at bridge piers. To establish the sensitivity of various parameters affecting sediment transport processes under ice, twenty tests were conducted in a refrigerated flume at the United States Army Corps of Engineers Cold Regions Research and Engineering Laboratory. All tests were conducted using a 5.08-cm-diameter circular bridge pier and sand with d_{50} = 0.13 mm with various discharges. Flow velocities were selected to focus primarily on clear-water scour using both smooth and rough simulated ice covers for three surface conditions: open water, floating cover where the ice was free to respond to changes in water level, and a fixed cover simulating ice frozen to the pier and banks with a hydrostatic head created by an upstream ice jam.

The cover roughness and pressure flow condition both alter velocity distribution and caused live-bed scour even when the mean flow velocity, V_{avg}, was less than the critical velocity for bed movement, V_c. The combination of increased cover roughness and pressure flow resulted in the largest scour depth. This paper presents a summary of the field investigations and laboratory experiments, and discusses both the velocity distributions and shear stress analysis.

1. Introduction

The influence of an ice cover on a channel involves complex interactions among the ice cover, ice roughness, fluid flow, sediment, bed geometry, water depth, and channel geometry. This complex interaction can have a dramatic effect on sediment transport process and channel development, especially in narrow rivers. The extent of the ice cover's rigid influence is defined using the characteristic length, l, which is primarily a function of the ice cover thickness. For freshwater ice and a short-term, elastic load, the characteristic length is defined by $16h^{3/4}$, where h is the ice thickness (Gold, 1971). The ice cover's rigid influence is known as the radius of influence and is approximately four to five times the characteristic length (Nevel, 1978). For example, 50-cm-thick ice has a corresponding l of 9.5 m, and the radius of influence from a pier or shoreline is 47.5 m. If the river is less than 95 m wide, the ice cover will be constrained from responding to changes in water levels. Restraining the ice cover may cause a condition akin to pressure flow, especially when the ratio between the unrestrained length (defined as the distance between shores or bridge piers and shores) and $10l$ decreases. In these cases, the river bed may experience ice-induced scour.

When the ice cover is frozen to the riverbanks and bridge piers, it restrains the cover from freely responding to changes in discharge conditions. The ice cover forms at the stage corresponding to the freeze-up discharge, defining the surface elevation and subsequently the flow area for the remainder of the winter. Any increase in the discharge above this freeze-up datum has to be accommodated by an increase in velocity. An ice cover approximately doubles the wetted perimeter of the river, adding to the flow resistance. Conveying a similar open-water discharge under the ice cover requires an increase in stage, mean velocity, or both.

For shallow rivers with thick ice, the change in discharge required to trigger break-up maybe an order of magnitude greater than the freeze-up discharge. A rule of thumb is that the corresponding open water stage has to increase two to four times the ice thickness to initiate break-up of the ice cover (Donchenko, 1975). Furthermore, if the discharge is above the freeze-up datum, but below the break-up threshold, the bed will continue to erode to restore the balance between the shear stress and the erodibility of the bed material. Roughness on the underside of the ice also has a role in the scour process.

Although ice impacts on sediment transport can be significant in cold regions, the effect of a fixed ice cover has yet to be considered in scour and sediment transport processes.

2. Revised Bridge Scour Model

The scour process and resulting scour hole depth are a function of several factors that can be grouped into four major categories: flow, bed sediment, bridge geometry, and time. As defined by Melville and Coleman (2000), the functional relationship between the depth of scour, d_s, and its dependent parameters is

$$d_s = f\,[\text{Flow } (\rho, \nu, V, y, G, g), \text{ bed sediment } (d_{50}, \sigma_g, \rho_s, V_c), \text{ bridge geometry (B, Sh, Al), time (t)}] \quad [1]$$

where

ρ = fluid density
ν = fluid viscosity
V = mean approach flow velocity
y = flow depth

G = parameter describing effects of lateral distribution of flow in the approach channel
g = acceleration due to gravity
d_{50} = median size of sediment
σ_g = geometric standard deviation of sediment particle size distribution
ρ_s = sediment density
V_c = critical mean approach flow velocity for entrainment of bed sediment
B = foundation width = b = pier width
Sh = shape factor
Al = alignment factor
t = time

To simplify the analysis, assume a constant relative density of sediment and the absence of viscous effects, which is typical for high Reynolds number flows. Eq (1) can then be non-dimensionalized and expressed as (Melville and Coleman, 2000)

$$\frac{d_s}{b} = f\left(\frac{V}{V_c}, \frac{y}{b}, \frac{b}{d_{50}}, \sigma_g, Sh, Al, G, \frac{Vt}{b}, \frac{V}{\sqrt{gb}}\right) \quad [2]$$

In addition to the increased wetted perimeter and boundary roughness, the fixed ice cover condition introduces a pressure flow condition. The increase in resistance cannot cause an increase in flow depth in the vicinity of the pier since the ice cover fixes the water surface elevation for some distance, L_c, upstream. To account for the pressure condition and the length of the fixed cover, two parameters, the difference between the approach depth (y_a) and depth under the fixed cover (y), y_h, and the length of fixed cover, L_c, must be included in Eq (1). Eq (1) is modified to yield Eq (3):

$d_s = f$ [Flow (ρ, ν, V, y, G, g, y_h), bed sediment (d_{50}, σ_g, ρ_s, V_c, k_{bed}), bridge geometry (B, Sh, Al), time (t), cover (k_{cover}, L_c)] [3]

Eq (2) can be modified to include a relative depth term, y_h/y, and a relative length-to-depth-ratio term, L_c/y, included in Eq (4):

$$\frac{d_s}{b} = f\left(\frac{V}{V_c}, \frac{y}{b}, \frac{b}{d_{50}}, \sigma_g, Sh, Al, G, \frac{Vt}{b}, \frac{V}{\sqrt{gb}}, \frac{k_{\text{cover}}}{k_{\text{bed}}}, \frac{y_h}{y}, \frac{L_c}{y}\right) \quad [4]$$

These terms provide a way to quantify the effect of the pressure head and extent of the fixed ice cover condition. The effect of pressure head was evaluated in this study. The effect of the fixed ice cover length upstream was not investigated in this study and was mitigated by extending the fixed cover far enough upstream to ensure uniform flow conditions approaching the pier. The effect of the extent of the ice cover remains a future research effort.

3. Field Investigations

The investigation into scour under ice was triggered by the collapse of a bridge over the White River in White River Junction, Vermont. During its service life the bridge survived more dramatic ice and flood events than the one that led to the failure of the pile foundation. The anecdotal evidence indicated that the foundation had deteriorated because of multiple bridge pier

scour cycles (Zabilansky, 1996). The first step to correlate the hydraulic and ice conditions with the scour process required the development of a robust real-time scour monitor that could operate in ice-covered rivers. The resulting instrumentation developed at CRREL utilized Time Domain Reflectometry (TDR) technology (Zabilansky and Yankielun, 2000). Three TDRs were installed upstream of a bridge pier in the White River. These measurements were augmented with the hydraulic, meteorological data and visual documentation of the ice conditions. Several years of measurements demonstrated the dramatic effect an ice cover has on sediment processes, especially during the rising limb of the break-up hydrograph.

The unique TDR instruments were incorporated into two additional projects to monitor sediment transport process during the winter: the Missouri River in eastern Montana and the Mississippi River near Rock Island, Illinois. Zabilansky (2002) summarized the observations from the three case studies, which help define the following test parameters and provided validation data for the flume study described below. Moreover, preliminary findings from an ongoing study indicate that scour under ice was a contributing factor in the collapse of the I-90 Bridge over the Schoharie Creek on April 5, 1987.

4. Experimental Study

This investigation was designed primarily as a sensitivity analysis to determine the effects of two critical parameters on the sediment transport process: pressure flow and ice cover roughness. Pressure flow is assumed to occur when the ice cover is fixed. The depth of scour around a model cylindrical bridge pier and the velocity profiles were used to assess the influence of these parameters. All tests were designed to be in the clear-water scour regime, where the mean velocity, V_{avg}, was less than critical velocity, V_c, defined as the threshold for general bed movement. Table 1 lists the general testing conditions in terms of the cover condition and relative cover roughness for the twenty tests that were conducted.

TABLE 1. Test conditions.

Number of Tests	Cover Condition	Relative Cover Roughness
6	Open Water/ Free Surface	N/A
5	Floating	Smooth
1	Floating	Rough
6	Fixed	Smooth
2	Fixed	Rough

The apparatus used in this study is the recirculating tilting bed flume, housed in a coldroom in the Ice Engineering Facility at CRREL. The flume is 36.58 m long, 1.22 m wide, and 0.61 m deep and can be tilted from a +1° to a –2° slope. To avoid experimental effects caused by variations in thermally grown ice covers, simulated ice with stable engineering properties was used, rather than an ice cover created using the room's refrigeration system. The water temperature was maintained at 1.6°C to obtain values of density and viscosity typical of an ice-covered channel. Downstream of the entrance transition section, the flume was filled to a depth of 19.05 cm with uniform sand, with a median grain diameter of 0.13 mm and a sediment uniformity coefficient of 1.41. The ice cover was simulated using Styrofoam insulation panels, with the natural finish used as the smooth cover (with an estimated Manning's n of approximately 0.010). For the rough cover, a geotextile open mat (Enkamat, manufactured by Maccaferri) was attached to the Styrofoam. Manning's n for the rough cover is reported as 0.0303 (Maccaferri, 2002).

For the fixed cover tests, the simulated ice was fixed vertically for 15.24 m around the pier (12.19 m upstream to 3.05 m downstream) to maintain a water depth of 22.86 cm. To

simulate an upstream ice jam that creates a hydrostatic head under the fixed cover section, an 11.58-m-long transition section was extended immediately upstream of the fixed cover. The simulated ice in the transition section followed a linear slope from the fixed elevation to the hydrostatic head elevation.

5. Velocity Distribution Analysis

Velocity measurements were taken 3.66 m upstream of the pier on the centerline and at locations 25.5 cm left and right of the centerline. The vertical velocity profiles were taken using a two-dimensional Acoustic Doppler Velocimeter (ADV) with a 1-s sample rate for two minutes at 1-cm increments between the bed and the water surface or underside of the cover. A complete description of the experimental set-up and procedure can be found in Hains and Zabilansky (2004) and Hains (2004).

The analyses were conducted by normalizing the average velocity by the critical velocity, which for this sediment is 27.43 cm/s. The majority of tests were conducted at a relative velocity of 0.8589, and it is at this relative velocity that the effects of the different cover and pressure conditions can be most readily identified. A discussion of the full test series can be found in Hains (2004).

The effects of ice cover roughness on the velocity profile are evident in Figure 1. As expected, the open water profile is logarithmic. For the floating smooth cover, the profile is gradual, with the maximum velocity approximately at the mid-depth, indicating that the roughness of the Styrofoam and bed are similar. For the floating rough cover, the maximum velocity is also at mid-depth but is about 20% greater than the smooth ice profile. The steeper velocity gradient is responsible for the live-bed scour that was observed under the rough floating cover. The effects of the pressurized flow condition are not significant when the smooth ice cover is fixed (Fig. 2). Here, the depth of flow on the ordinate axis has been non-dimensionalized to allow comparisons between tests with different depths of flow.

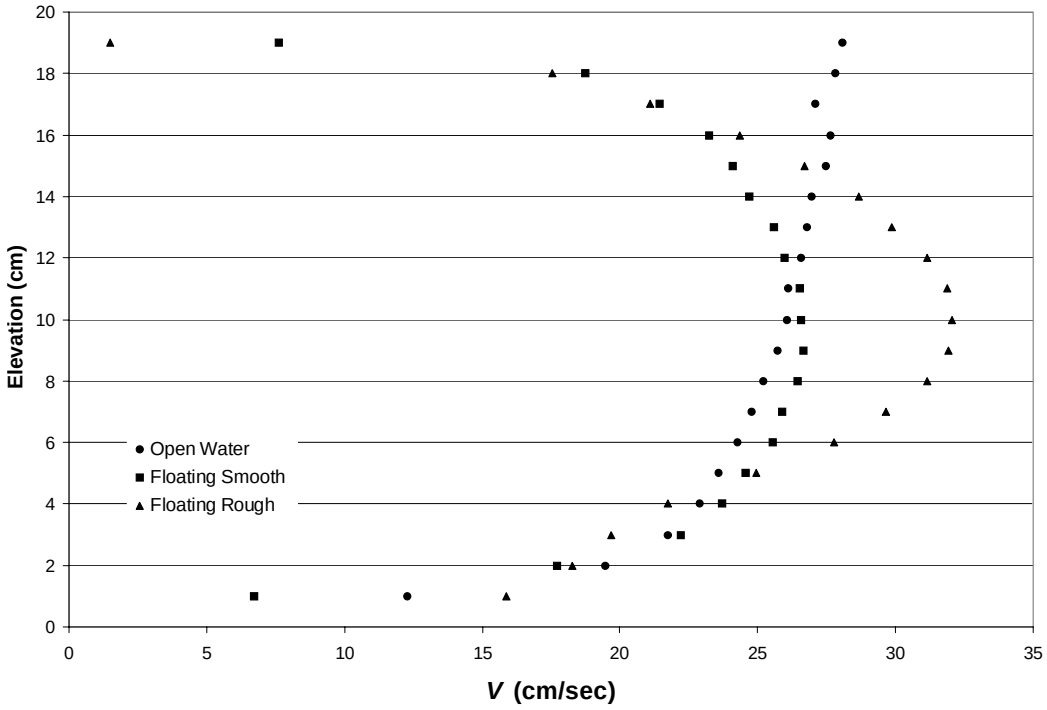

FIGURE 1. Velocity profiles for open water and floating smooth and rough ice covers. V_{avg} = 23.56 cm/s, V_{avg}/V_c = 0.8589.

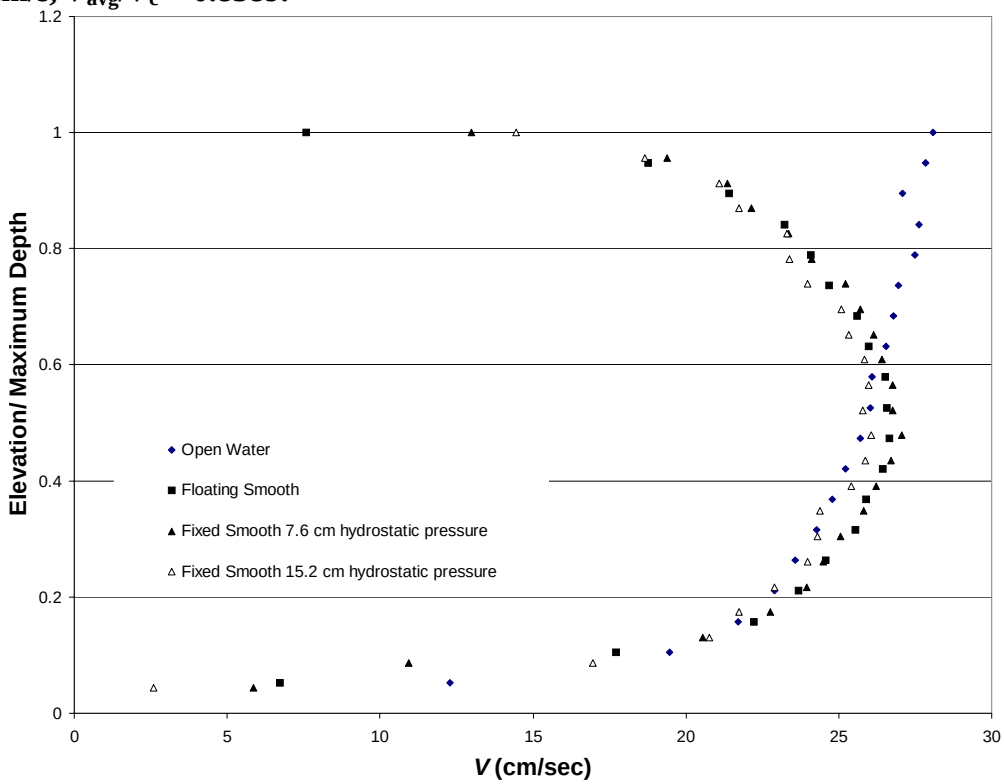

FIGURE 2. Velocity profiles for open water and floating and fixed smooth ice covers with hydrostatic heads of 7.6 and 15.2 cm. V_{avg} = 23.56 cm/s, V_{avg}/V_c = 0.8589.

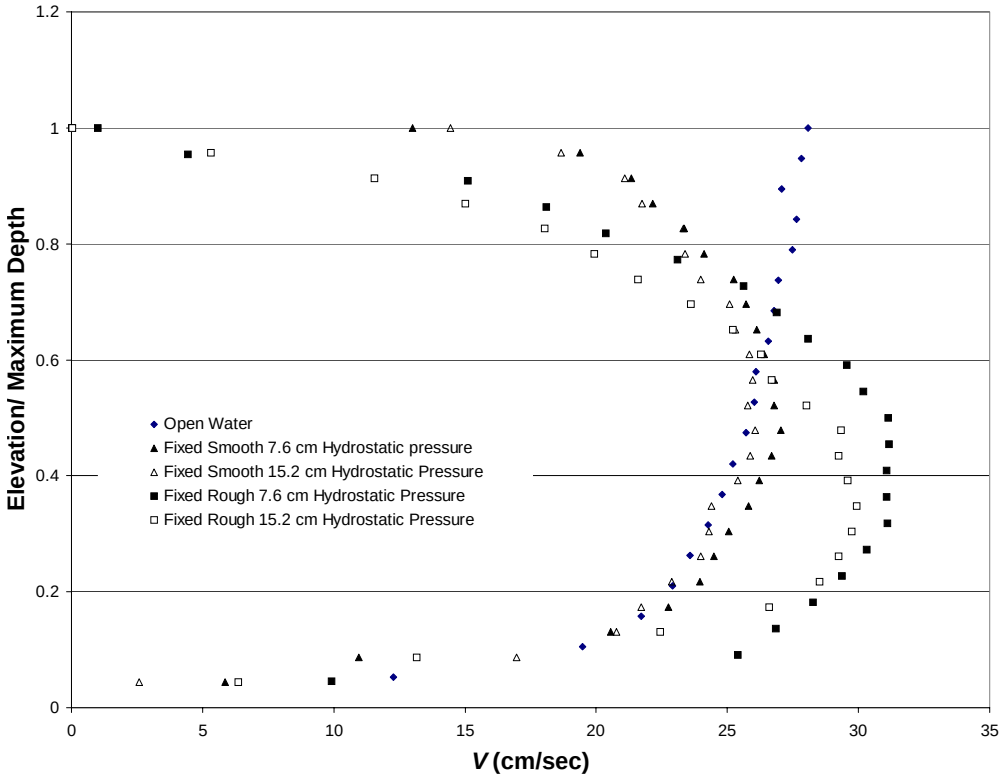

FIGURE 3. Velocity profiles for open water and fixed smooth and rough ice covers with hydrostatic heads of 7.6 and 15.2 cm. V_{avg} = 23.56 cm/s, V_{avg}/V_c = 0.8589.

More significant changes in the velocity profile are observed with a fixed rough cover (Fig. 3). The maximum velocity for the fixed cover with the pressurized condition was higher than for the floating cover condition. For the smooth fixed cover tests, the velocity profile was nearly symmetrical about the mid-depth. The velocity profile for the rough fixed cover test shifted dramatically towards the bed, the smoother of the two boundaries. The steeper velocity gradient near the bed and the associated increased shear stresses along the bed resulted in live-bed scour.

The velocity profile shift toward the smooth cover is more pronounced when the relative velocity is increased to 0.9278, and it is especially pronounced for the higher pressure head (Fig. 4). Moreover, at this relative velocity, the maximum velocity for both pressurized tests was greater than those of the floating cover tests. The live-bed scour that occurred under these test conditions is likely a result of the greater maximum velocity.

Theoretically, V_{avg}/V_c must be greater than one for live-bed scour to occur for the open water condition. However, these test results indicate that, although the average velocity may be an acceptable indicator for the type of scour (clear-water versus live-bed) for open water conditions, it is not acceptable for ice-covered water, especially when a pressurized or rough cover exists. Figure 5 demonstrates this point with the velocity profiles for the floating and fixed rough covers. As the hydrostatic pressure increases from zero in the floating condition to 15.2 cm in the fixed condition, the velocity profile shifts towards the smoother boundary. This profile shift will subject the bed to higher shear stresses and accelerated scour.

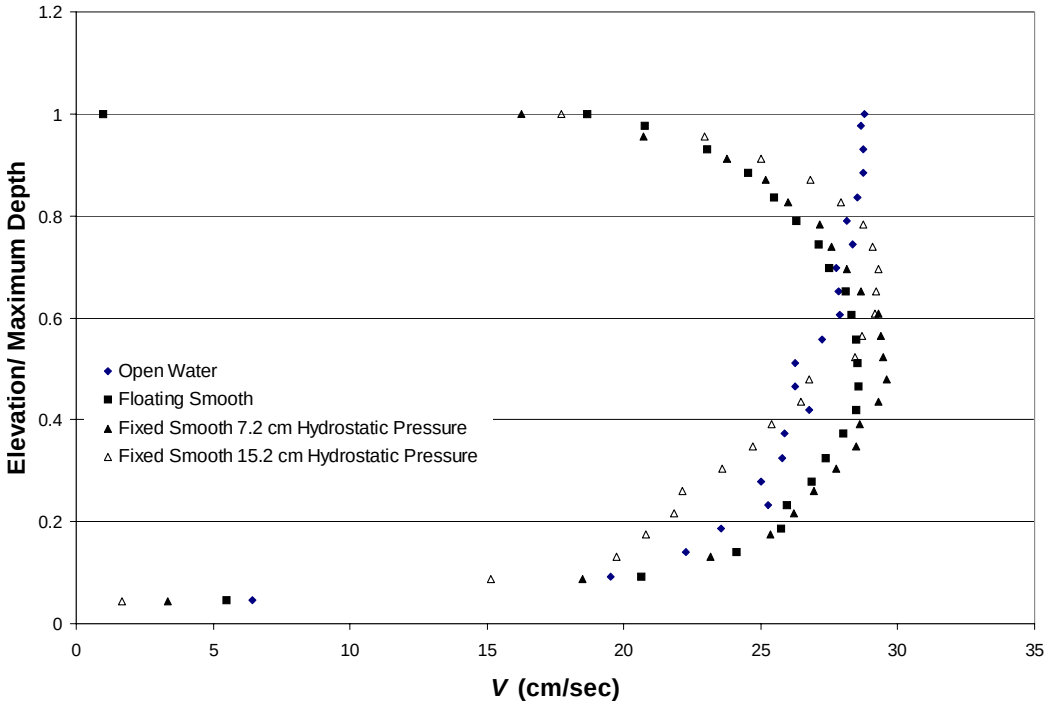

FIGURE 4. Velocity profiles for open water and floating smooth and fixed smooth ice covers with hydrostatic heads of 7.6 and 15.2 cm. V_{avg} = 25.48 cm/s, V_{avg}/V_c = 0.9278.

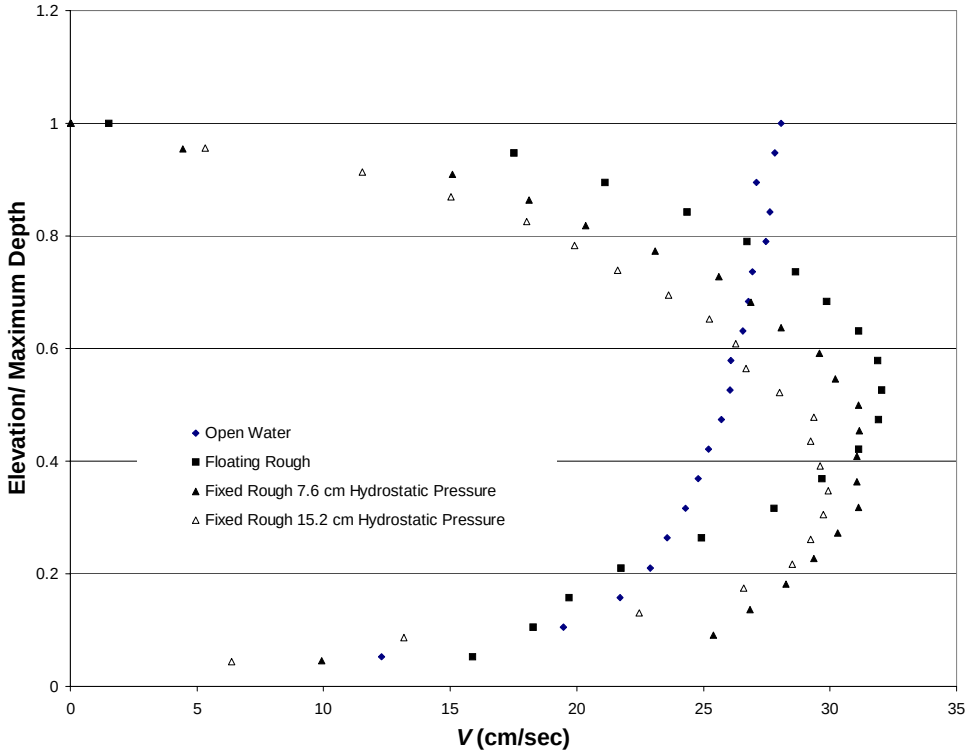

FIGURE 5. Velocity profiles for open water and restrained smooth and rough ice covers with hydrostatic heads of 7.6 and 15.2 cm. V_{avg} = 23.56 cm/s (0.773 fps), V_{avg}/V_c = 0.8589.

6. Shear Stress Analysis

Although critical average velocity is often used to characterize the type of channel scour, a more fundamental approach is to examine the shear stress which is directly used to quantify resistance to motion. When the critical shear stress of sediment particles on the bed is exceeded, particles move. Shear stress is a measure of the resistance to flow and, when determined upstream of a bridge pier, may be used as an indicator for the depth of scour at the pier. This section presents the analysis of the shear stresses on the bed and on the cover as determined from the velocity profiles 3.66 m upstream of the bridge pier.

With a median sediment size, d_{50} = 0.13 mm and water at 35° F, the Shield's diagram yields a boundary Reynolds number of 1.3 at critical conditions defined as incipient motion. Based on the definition of boundary Reynolds number in Eq. 5,

$$R_* = \frac{U_* d}{\nu} \qquad [5]$$

where

U_* = shear velocity
ν = fluid viscosity
d = characteristic length = d_{50} = median size of sediment

the critical shear velocity is 0.016 m/s. The shear velocity is related to average shear stress by Eq. 6.

$$U_* = \sqrt{\frac{\tau_o}{\rho}} \qquad [6]$$

Thus,

$$\tau_o = \rho U_*^2 \qquad [7]$$

At 35° F, the density of clear water is 1.0004 x 10^3 kg/m^3 and the critical shear stress is 0.2561 N/m^2.

In the vicinity of the boundary, it was assumed that the velocity distributions followed the logarithmic law of the wall (Tatinclaux and Gogus 1983). For a smooth boundary,

$$\frac{V(z)}{U_*} = \frac{1}{\kappa} \ln\left(\frac{9 U_* z}{\nu}\right) \qquad [8]$$

and for a rough boundary,

$$\frac{V(z)}{U_*} = \frac{1}{\kappa} \ln\left(\frac{30 z}{\nu}\right) \qquad [9]$$

where κ is von Karman's constant which is assumed to be 0.4 for clear water. Since the boundary Reynolds number is less than 5, the bed can be considered hydraulically smooth. For a hydraulically smooth boundary, the boundary layer includes a viscous sublayer.

A linear regression analysis of the measured velocity, $V(z)$ versus the ln z yielded the shear velocity from the slope of the regression line. More specifically, the slope of the regression line is U_* / κ. Although the no slip condition, $V(0) = 0$, is assumed at the boundary, this is mathematically impossible for the assumed logarithmic profiles since the logarithm is singular at zero. For the smooth bed boundary, the best-fit of the measured and calculated velocity profiles occurred when the z-origin was 0.0015 cm which is an order of magnitude less than the d_{50} of the sediment on the bed (0.013 cm). The same z-origin was also found to be the best-fit for the smooth cover which further indicates that the smooth cover and bed exhibit similar roughness characteristics. Hains (2004) contains the complete shear stress analysis for the bed and smooth cover.

For the rough boundary, the actual origin of the z-ordinate cannot be assumed to be close to boundary and must be determined by experimentation or by optimizing the correlation coefficient in the regression analysis (Tatinclaux and Gogus 1983). Gogus (1980) noted that the z-origin was located at approximately the average roughness height of the model cover. The Enkamat© geotextile used for the rough cover tests was approximately 10 mm thick. From the regression analysis, the z-origin for the rough covers varied from 0.5 cm to 0.8 cm which is within the thickness of the Enkamat ©. Also, for the rough covers, the equivalent sand grain roughness, k_s, can be determined from the intercept of the linear regression. Hains (2004) also contains the shear stress analysis performed for the rough covers.

For the open water tests, a majority of the velocity profile points were used in the linear regression. For the covered tests, the flow was divided into two regions at roughly the location of the maximum velocity. The bed region was analyzed in the same manner as in the open water tests; whereas, the velocity profile was inverted to examine the shear stress on the cover. Figure 6 is a definition sketch of the two regions.

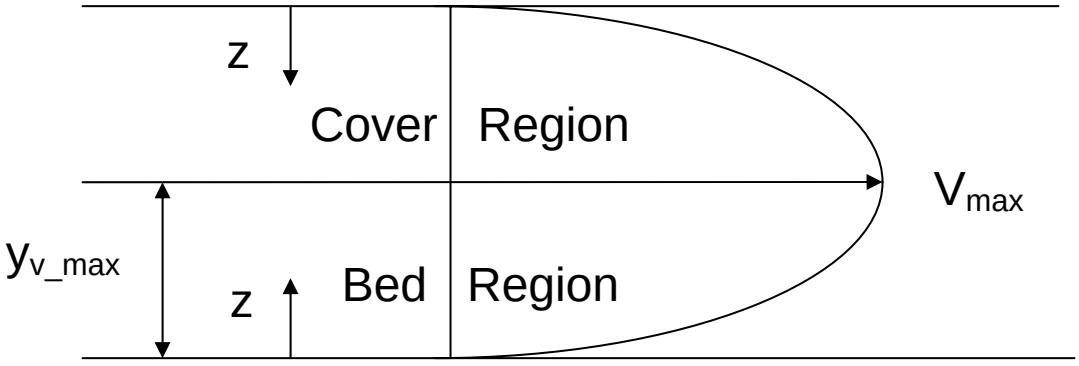

FIGURE 6. A General Shear Stress Analysis Definition Sketch.

Lau (1982) noted that the velocity profiles under floating covers deviate from the logarithmic distribution for about 40% of the flow depth. The velocity is less than that given by the logarithmic profile for approximately the 40% of the profile near the location of the maximum velocity (Lau 1982). Consequently, for the regression analysis of the covered flows, approximately the lower 30% of profile was used for the bed shear stress analysis and the upper

30% used for the cover shear stress analysis. Finally, since the boundary interfered with the velocity measurement near the boundary, the closest two points to the boundary were not used in the regression analysis. This gave a much better fit of the data.

Table 2 lists the test series notation and Table 3 lists the computed bed shear stress and other data from the linear regression analysis of the velocity profiles.

TABLE 2. Test Series Notation

Notation	Cover Condition	Relative Cover Roughness
A	Open Water/Free Surface	N/A
B	Floating	Smooth
R	Floating	Rough
C	Fixed	Smooth
XR	Fixed	Rough

TABLE 3. Bed Shear Stress Results.

Test	d_s [cm]	Slope	U_* [cm/sec]	τ [N/m^2]	r^2
V = 0.650 fps, V_{avg}/V_c = 0.7222					
A5	6.826	2.3448	0.9379	0.0880	0.9826
B3	6.985	2.6038	1.0415	0.1085	0.9977
V = 0.700 fps, V_{avg}/V_c = 0.7777					
A6	7.144	2.6168	1.0467	0.1096	0.9951
B5	8.255	2.8418	1.1367	0.1293	0.9953
V = 0.735 fps, V_{avg}/V_c = 0.8167					
A3	6.826	2.7342	1.0937	0.1197	0.9970
B1	8.255	2.8351	1.1340	0.1287	0.9968
C1	7.938	2.8253	1.1301	0.1278	0.9963
C4	7.938	2.6947	1.0779	0.1162	0.9950
V = 0.773 fps, V_{avg}/V_c = 0.8589					
A2	8.096	2.9558	1.1823	0.1398	0.9984
B2	8.255	3.1695	1.2678	0.1608	0.9997
R1*	7.620	3.2730	1.3092	0.1715	0.9169
C5	8.255	2.9800	1.1920	0.1421	0.9914
C6	8.096	2.8760	1.1504	0.1324	0.9951
XR1*	7.303	3.6280	1.4512	0.2107	0.9988
XR2*	8.414	3.4487	1.3795	0.1904	0.9786
V = 0.836 fps, V_{avg}/V_c = 0.9278					
A4	8.414	3.0382	1.2153	0.1477	0.9967
B4	8.573	3.2361	1.2944	0.1676	0.9993
C2*	8.255	3.2803	1.3121	0.1722	0.9950
C3*	7.303	2.8328	1.1331	0.1284	0.9796

* Denotes live-bed scour

As the relative velocity increases, the bed shear stress increases. For each relative velocity value, the bed shear stress under the floating cover was greater than that under the open water condition. The depth of scour under the floating cover condition was also greater than that under the open water condition. For the smooth cover, the bed shear stresses were less than that under the floating cover and decreased with an increase in pressure head. The depths of scour follow a similar trend.

Although the shear stress analysis was performed for the live-bed scour, these values are approximate and only account for the surface resistance. The dunes that are indicative of live-bed scour provide additional form resistance. By definition, in live-bed scour, the shear stress on the bed must exceed the critical shear stress. The correlation coefficients for the linear regression on these profiles are much lower than those of the clear-water scour tests. Therefore, the z-origin must be increased for these tests resulting in a much steeper slope and larger shear stress. However, with a larger z-origin, the assumed velocity profile is no longer valid. Consequently, the only definitive conclusion for the shear stress analysis for the live-bed scour test is that the critical shear stress was exceeded.

Table 4 lists the shear stress on the underside of the simulated ice cover and computed data from the linear regression of the velocity profiles in the cover flow region.

TABLE 4. Cover Shear Stress Results.

Test	d_s [cm]	Slope	U_* [cm/sec]	τ [N/m^2]	r^2
V = 0.650 fps, V_{avg}/V_c = 0.7222					
B3	6.985	2.5401	1.0160	0.1033	0.9938
V = 0.700 fps, V_{avg}/V_c = 0.7777					
B5	8.255	2.7946	1.1178	0.1250	0.9934
V = 0.735 fps, V_{avg}/V_c = 0.8167					
B1	8.255	2.7910	1.1164	0.1247	0.9972
C1	7.938	2.8196	1.1278	0.1273	0.9954
C4	7.938	2.7590	1.1036	0.1218	0.9919
V = 0.773 fps, V_{avg}/V_c = 0.8589					
B2	8.255	3.0521	1.2208	0.1491	0.9918
R1**	7.620	11.1850	4.4740	2.0025	0.9970
C5	8.255	2.9574	1.1830	0.1400	0.9941
C6	8.096	2.8788	1.1515	0.1327	0.9959
XR1**	7.303	10.8480	4.3392	1.8836	0.9940
XR2**	8.414	10.6120	4.2448	1.8026	0.9923
V = 0.836 fps, V_{avg}/V_c = 0.9278					
B4	8.573	3.1779	1.2712	0.1616	0.9948
C2*	8.255	3.2721	1.3088	0.1714	0.9972
C3*	7.303	3.3489	1.3396	0.1795	0.9853

* Denotes live-bed scour

** Denotes live-bed scour and rough cover

As the relative velocity increases, the shear stress on the underside of the cover increases. However, as the pressure head is increased, the shear stress on the underside of the smooth covers decreases slightly for a relative velocity of 0.8167 and 0.8589. For a relative velocity of

0.9278, the shear stress on the underside of the cover increased when the pressure head was increased and at this relative velocity, the shear stress on the underside of the cover was greater under the pressurized flow condition than that under the floating cover.

For the rough cover, in addition to determining the shear stress on the underside of the cover, the equivalent sand grain roughness, k_s, of the cover can be calculated from the intercept, y', of the linear regression analysis of the velocity profile according to the equation (Gogus 1980):

$$\ln k_s = -\frac{0.4y'}{U_*} + \ln 30 \qquad [10]$$

With k_s, an approximate Manning's n for the rough cover can be calculated from Strickler's equation (Chow 1959):

$$n = 0.0342 k_s^{1/6} \qquad [11]$$

where k_s is in feet. Table 5 lists the z-origin, intercept (y'), equivalent sand grain roughness (k_s), and Manning's n for each of the rough cover tests.

TABLE 5. Rough Cover Roughness Analysis.

Test	z-origin [cm]	y' [cm/sec]	k_s [cm]	Manning's n
R1	0.50	8.2494	14.35	0.030
XR1	0.65	3.9007	20.94	0.032
XR2	0.80	3.2853	26.72	0.034

The k_s values are quite large, and in the case of XR2, greater than the 22.86 cm depth of flow under the cover. However, these results are consistent with the smooth bed and cover tests conducted by Gogus (1980) in his study of flow between two boundaries of unequal roughness. The rough cover in Gogus' (1980) tests consisted of plastic blocks randomly distributed over a molten paraffin base on sheet-metal panels. The average roughness height of the rough cover in Gogus' tests was 10 mm, similar to the Enkamat© geotextile. In this study, the calculated values of k_s exceeded the depth of flow for the rough cover and smooth bed tests. Gogus (1980) noted that "the equivalent sand grain roughness is one order of magnitude greater than the actual roughness height, in accordance with the results of previous experiments on surfaces with large, irregular, randomly distributed roughness elements." Further, Chow (1959) states that

> It should be noted that the roughness height is merely a measure of the linear dimension of the roughness elements but is not necessarily equal to the actual, or even an average, height. For example, two roughness elements may have different linear dimensions, but owing to the difference in shape and orientation, they may produce identical roughness effect, and thus, their roughnesses will be designated by the same roughness height.

Finally, the Manning's n values in the table are consistent with the Manning's n value of 0.0303 reported by Maccaferri Engineering for the Enkamat© geotextile.

7. Conclusion

The field observations and flume study indicate that river ice is an active participant in the scour and sediment transport process in cold regions. The roughness of the ice cover and the pressurized flow condition strongly influences the velocity distribution of the flow and must be considered in the analysis of scour and sediment transport in ice-covered rivers. Under the influence of a rough cover and pressurized flow, the velocity profiles shift toward the smoother boundary. When the underside of the ice cover is rougher than the bed, the velocity profile shift causes live-bed scour at average velocities less than the critical velocity. If the ice cover forms from dynamic processes, typical of steep, narrow rivers in cold regions, the bottom surface of the ice may be rougher than the bed. When the discharge increases above the freezeup datum, the pressurized flow condition, combined with the rough underside of the ice, will cause the maximum velocity in the flow to both increase and shift closer to the bed. The result will be increased shear stresses on the bed, increased bed erosion and greater depths of scour at bridge piers.

Clearly additional research is required to quantify effects of pressure and roughness on the velocity profiles, shear stresses, bed erosion, scour at bridge piers and sediment transport. The complex nature of the ice, flow, and sediment interaction requires a laboratory flume study to further characterize the effects of the pressure and roughness of the ice cover.

References

Chow, V.T. 1959. *Open Channel Hydraulics.* McGraw-Hill, NY.

Donchenko, R. V. 1975. *Conditions for Ice Jam Formation in Tailwaters.* Draft Translation 669, U.S. Army Cold Regions Research and Engineering Laboratory, Hanover, NH.

Gogus, Mustafa 1980. "*Flow Characteristics Below Floating Ice Covers with Applications to Ice Jams*." Ph.D. Dissertation, The University of Iowa, Iowa City, IA.

Gold, L. W. 1971. "Use of Ice Covers for Transportation." *Canadian Geotechnical Journal*. *8*: 170–181.

Hains, D. B. 2004. "An Experimental Study of Ice Effects on Scour at Bridge Piers." Ph.D. Dissertation, Lehigh University, Bethlehem, PA.

Hains, D. B., and L. J. Zabilansky. 2004. *Laboratory Test of Scour under Ice: Data and Preliminary Results*. Technical Report TR-04-9, U.S. Army Cold Regions Research and Engineering Laboratory, Hanover, NH. Available at http://www.crrel.usace.army.mil/techpub/CRREL_Reports/reports/TR04-9.pdf

Hains, D., L. J. Zabilansky, and R. N. Weisman. 2004. "An Experimental Study of Ice Effects on Scour at Bridge Piers." In *Cold Regions Engineering and Construction Conference and Expo 2004* (16–19 May, 2004, Edmonton, Alberta).

Lau, Y. L. 1982. "Velocity Distributions Under Floating Covers." *Canadian Journal of Civil Engineering*. 9: 76-83.

Maccaferri Engineering. 2002. "Macra 1 2002 Hydraulic Channeling Design Software- Help File."

Melville, Bruce W. and Stephen E. Coleman. 2000. *Bridge Scour.* Water Resources Publications, LLC, Highlands Ranch, CO.

Nevel, D. E. 1978. *Bearing Capacity of River Ice for Vehicles*. Technical Report CR78-03, U.S. Army Cold Regions Research and Engineering Laboratory, Hanover, NH.

Tatinclaux, Jean-Claude and Mustafa Gogus. 1983. "Asymmetric Plane Flow with Application to Ice Jams." *Journal of Hydraulic Engineering.* 109: 1540-1554.

Zabilansky, L. J. 1996. *Ice Force and Scour Instrumentation for the White River, Vermont*. Special Report 96-6, U.S. Army Cold Regions Research and Engineering Laboratory, Hanover, NH.

Zabilansky, L. J. 2002. "Ice Cover Effects on Bed Scour: Case Studies." *Proceedings, 11th ASCE Cold Regions Engineering* (19–23 May 2002, Anchorage, AK).

Zabilansky, L. J., and N. E. Yankielun. 2000. "Measuring Scour Under Ice in Real Time." *Proceedings of the Transportation Research Board Meeting 2000*, TRB ID 00-420 (12–14 January 2000, Washington, DC).

Zabilansky, L. J., R. Ettema, N. E. Yankielun, and J. L. Wuebben. 2002. Survey of River-Ice *Influences on Channel Stability along the Fort Peck Reach of the Missouri River, Montana, Winter 1998–1999*. Technical Report TR-02-14, U.S. Army Cold Regions Research and Engineering Laboratory, Hanover, NH. Available at http://www.crrel.usace.army.mil/techpub/CRREL_Reports/reports/TR02-14.pdf